CHEMISTRY
A EUROPEAN JOURNAL

DOI: 10.1002/chem.201000403

Synergistic Behavior of Bimetallic Rhenium Cluster Catalysts: Spectroscopic Investigation into the Nature of the Active Site

Enrica Gianotti,*[a] Vasudev N. Shetti,[a] Maela Manzoli,[a] Jonathan A. L. Blaine,[b] William C. Pearl, Jr.,[c] Richard D. Adams,[c] Salvatore Coluccia,[a] and Robert Raja*[b]

Abstract: Single-site Re nanoparticles were produced by anchoring dirhenium organometallic clusters on to the inner walls of mesoporous silica. The presence of oxophilic atoms (Sb or Bi) is essential to obtain well dispersed Re^0 centers. The interaction between the organometallic cluster and the silica support is critical for the generation of well-defined and isolated Re^0 single sites. FTIR spectroscopy was used to track the decomposition of the organometallic precursors and the adsorption of probe molecules such as CO on the metal sites sheds valuable information on the catalytic potential of this new class of bimetallic nanocatalysts.

Keywords: ammoxidation · nanoparticles · CO adsorption · FTIR spectroscopy · rhenium

Introduction

Rhenium-based materials are widely used as catalysts in many industrial processes such as metathesis of alkanes and selective hydrogenation of organic compounds.[1,2] Only a few applications of these catalysts in selective oxidations have been reported.[3–5] Recently, several studies have revealed that combinations of rhenium and antimony exhibit catalytic activity for the ammoxidation of certain hydrocarbons.[6–8] Further, anchoring Re–organometallic complexes or Re–oxo species on inorganic supports renders them stable at high-temperature reaction conditions.[9,10] In particular, bimetallic nanocluster systems based on rhenium, which when combined with oxophiles, such as antimony or bismuth, can be used to generate highly dispersed nanoparticle catalysts for the ammoxidation of 3-picoline to nicotinonitrile (precursor for niacin) under mild conditions in the liquid phase.[11] These catalysts are compositionally simple nanoparticles of Re and either Sb or Bi, that exhibit considerable synergy between the constituent elements and are produced by supporting dirhenium–organometallic complexes ($[Re_2(CO)_8(\mu\text{-}SbPh_2)(\mu\text{-}H)]$, $[Re_2(CO)_8(\mu\text{-}SbPh_2)_2]$, and $[Re_2(CO)_8(\mu\text{-}BiPh_2)_2]$) on mesoporous silica, followed by subsequent removal of the carbonyl ligands by gentle thermolysis under vacuum. The interaction of the clusters with the inorganic silica support strongly affects the nature and the dispersion of the metal active sites that are produced after the decomposition of the precursor for the generation of single-site, multinuclear, bimetallic, heterogeneous catalysts. To understand the catalytic performance, it is important to clarify and elucidate how the organometallic precursors are decomposed at increasing temperatures and how the active sites are generated.

In this study, thermogravimetric analysis (TGA) and in situ FTIR spectroscopy were used to follow the decomposition of three different rhenium-containing organometallic precursors and the subsequent anchoring of the resulting nanoclusters on the support. We have observed that the temperature and surrounding environment at which the cluster precursors are decomposed is critical for the anchoring and subsequent generation of highly active and selective rhenium-based nanoparticles (Re_2Sb, Re_2Sb_2, and Re_2Bi_2) that function as single-site, heterogeneous catalysts for the liquid-phase ammoxidation of 3-picoline to nicotinonitrile. In order to further investigate the nature, dispersion, and

[a] Dr. E. Gianotti, Dr. V. N. Shetti, Dr. M. Manzoli, Prof. S. Coluccia
Department of Chemistry IFM and NIS-Centre of Excellence
University of Turin, V. P. Giuria 7, 10125 Turin (Italy)
Fax: (+39) 011-6707953
E-mail: enrica.gianotti@unito.it

[b] J. A. L. Blaine, Prof. R. Raja
School of Chemistry, University of Southampton
Highfield, Southampton SO17 1BJ (UK)
Fax. (+44) 2380593781
E-mail: rr3@soton.ac.uk

[c] W. C. Pearl, Jr., Prof. R. D. Adams
Department of Chemistry & Biochemistry
University of South Carolina, Columbia SC 29208 (USA)

Supporting information for this article is available on the WWW under http://dx.doi.org/10.1002/chem.201000403.

oxidation state of the metal sites exposed at the catalyst surface, CO was used as molecular probe and was adsorbed on the activated catalysts at room temperature. CO is able to interact directly with the metal nanoparticles, producing typical bands in the carbonyl stretching region ($\tilde{\nu}=2200$–$1700\,cm^{-1}$); by studying their intensity, the positions of the maxima, and their behavior on outgassing, it is possible to obtain useful insights that help to clarify the nature of the metal active sites.

The main objectives of this paper are aimed at providing a detailed spectroscopic understanding of the nature of the active sites that have led to the synergistic enhancements in the catalytic ammoxidation of 3-picoline (for the preparation of vitamin B3). Hence, it is of fundamental importance in this study to mimic the same experimental conditions that were employed in the earlier Communication.[11] Therefore, it is imperative that the active sites characterized in this study were subject to the same thermal treatments to that of the "working catalyst" in order to arrive at structure–property correlations.

Results and Discussion

Ammoxidation of 3-picoline: The three new Re-based nanocluster catalysts (hereafter denoted as Re_2Sb, Re_2Sb_2, and Re_2Bi_2) were derived from the organometallic precursor complexes: $[Re_2(CO)_8(\mu\text{-}SbPh_2)(\mu\text{-}H)]$, $[Re_2(CO)_8(\mu\text{-}SbPh_2)_2]$, and $[Re_2(CO)_8(\mu\text{-}BiPh_2)_2]$ (Figure 1) and were anchored onto a mesoporous silica support (pore diameter of 38 Å). The precursor cluster complexes were prepared as previously reported[11,12] and characterized by single-crystal X-ray diffraction analyses. The clusters shown in Figure 1B and C are isomorphous, isostructural, and centrosymmetrical. They each contain two MPh_2 ligands, M = Sb or Bi, that bridge two $Re(CO)_4$ groups. There is no metal–metal bond between the two rhenium atoms; Re···Re = 4.343(1) Å for B and 4.483(1) Å for C.

The effect of activation temperature on the liquid-phase ammoxidation of 3-picoline to nicotinonitrile was investigated by using the above three cluster complexes (Figure 2).

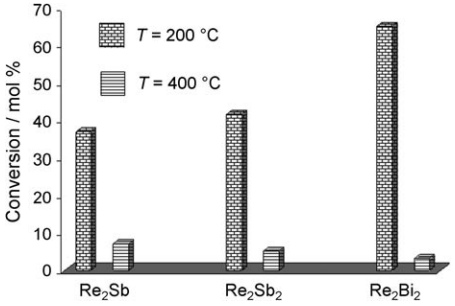

Figure 2. The effect of activation temperature and its influence on the catalytic activity in the ammoxidation of 3-picoline (see Experimental Section for reaction conditions).

All three catalysts displayed reasonable activities when activated at 200 °C (as is normally the case with anchored bimetallic nanocluster complexes).[11,13,14] In this study, however, higher activation temperatures were explored, as it was observed in previous studies[11] that the residual carbonyl ligands were still present on the activated catalyst at 200 °C. Also, in the same study,[11] it was noted that activation of $[Re_2(CO)_8(\mu\text{-}BiPh_2)_2]$ at higher temperatures (300 °C) leads to slightly enhanced catalytic behavior. Table 1 shows the conversions, turnover number (TON), and the product selectivity of the three cluster complexes used in this study together with the data of pure $[Re_2(CO)_{10}]/SiO_2$ and pure $[BiPh_3]/SiO_2$ for sake of comparison. The turnover numbers that we observe for this reaction are unprecedented (approaching nearly 10000) and this clearly indicates that residual carbonaceous species arising from the decomposition of the ligands activated at 200 °C are minimal, as this would have otherwise greatly retarded the overall activity of our catalysts. Furthermore, detailed X-ray emission spectroscopy and high-resolution TEM (HRTEM) of both the neat and the used catalysts (see Figure 4 of reference [11]) did not reveal the presence of any residual carbon. From the above, we can categorically rule out any additional ligand effects associated with the carbon presence.

Table 1. Ammoxidation of 3-picoline by using new rhenium-based nanocluster catalysts supported on silica.

Catalyst	Conv. [mol %]	TON	Product selectivity [mol %]				
			3-cyanopyridine (nicotinonitrile)	niacinamide	niacin	pyridine	others
Re_2	12.5	833	75.3	5.7	3.2	–	15.0
Re_2Sb	37.0	3273	78.9	3.5	3.0	4.3	10.5
Re_2Sb_2	41.5	4575	75.0	5.0	4.5	4.9	10.5
Re_2Bi_2	65.0	9196	75.0	8.8	6.9	–	9.5
Bi	7.9	296	43.4	4.5	–	–	51.9

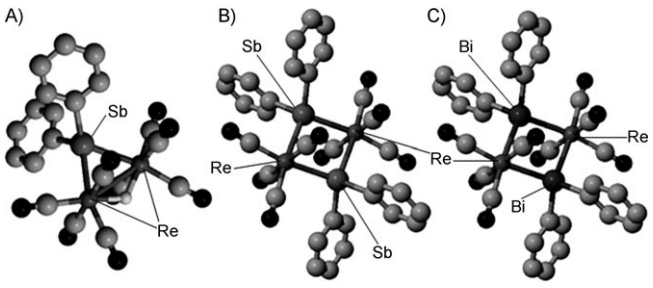

Figure 1. The precursor cluster complexes $[Re_2(CO)_8(\mu\text{-}SbPh_2)(\mu\text{-}H)]$ (A), $[Re_2(CO)_8(\mu\text{-}SbPh_2)_2]$ (B), and $[Re_2(CO)_8(\mu\text{-}BiPh_2)_2]$ (C) that were used for the ammoxidation of 3-picoline to nicotinonitrile. Phenyl hydrogen atoms are omitted for clarity.

Thermogravimetric analysis (TGA): The thermal decomposition of the organometallic precursors was followed by thermogravimetric analysis. The pure rhenium carbonyl, $[Re_2(CO)_{10}]$, anchored on mesoporous silica (hereafter denoted as Re_2) was also studied. The percentage weight loss of the as-synthesized samples, in the temperature range 25–500 °C, is reported in Figure 3. In most cases, the weight loss

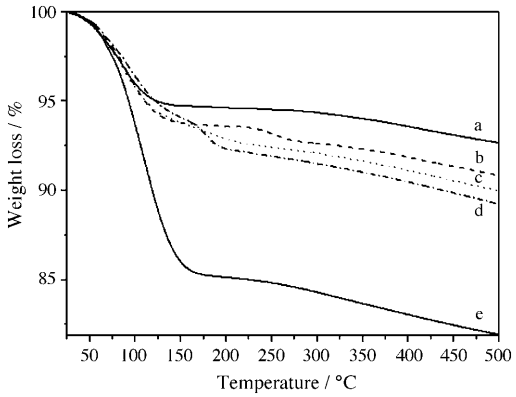

Figure 3. TGA analysis of $[Re_2(CO)_8(\mu\text{-}BiPh_2)_2]/SiO_2$ (curve a), $[Re_2(CO)_8(\mu\text{-}SbPh_2)_2]/SiO_2$ (curve b), $[Re_2(CO)_8(\mu\text{-}SbPh_2)(\mu\text{-}H)]/SiO_2$ (curve c), $[Re_2(CO)_{10}]/SiO_2$ (curve d), and pure SiO_2 (curve e).

is small (the maximum weight loss reaches about 10% in the case of $[Re_2(CO)_{10}]/SiO_2$, curve d), however, it is higher than the amount of organometallic precursor added to silica (3 wt%). This indicates that an additional weight loss, due to the desorption of water molecules from the porous silica, occurs between 25 °C and 150 °C and it represents the predominant contribution to the weight loss for all the as-synthesized samples. Beyond this temperature, the TG profiles smoothly decrease, indicating that the decomposition of the precursors is gradual. In particular, the $[Re_2(CO)_8(\mu\text{-}BiPh_2)_2]/SiO_2$ (curve a) shows the lowest weight loss, whereas in the case of $[Re_2(CO)_{10}]/SiO_2$ (curve d), the highest value is observed.

In Table 2, the percentage weight loss at 200 °C and at 400 °C is reported. Whilst it is possible that some residual ligands are still present at the former temperature, care was taken to ensure the complete decomposition of the organometallic precursors at the higher temperature. The trend shows that the weight loss decreases by the addition of oxophilic atoms to Re and by increasing of both the number of substituents (Re_2Sb to Re_2Sb_2) and atomic weight (from Sb to Bi). All the Re samples (Figure 3, curves a–d) show lower

Table 2. Wt% loss and calculated Δwt% at 200 °C and at 400 °C.

As-synthesized samples	wt% loss at 200 °C	Δwt% at 200 °C	wt% loss at 400 °C	Δwt% at 400 °C
Re_2	92.60	7.4	90.75	9.25
Re_2Sb	93.10	6.90	91.33	8.66
Re_2Sb_2	93.83	6.17	92.13	7.87
Re_2Bi_2	94.77	5.23	93.75	6.25

percentage weight loss with respect to the pure SiO_2 (Figure 3, curve e), especially in the 25–150 °C range, where the desorption of water molecules occurs. This means that the Re catalysts are less hydrophilic than SiO_2 and that a lower fraction of SiOH groups are available. This behavior confirms that SiOH groups are the ones on which the anchoring process occurs; in fact, as outlined above, the Bi-containing catalyst (Figure 3, curve a) shows the lowest weight loss at increasing temperature, meaning that an higher fraction of the organometallic complex is anchored on SiOH groups of the silica surface and suggesting a stronger interaction between the organometallic complex and the silica support.

FTIR characterization: To elucidate the interaction between the organometallic complexes and the silica support, FTIR spectroscopy was used to monitor the decomposition of the precursors at increasing temperature. The FTIR spectra of the thermal decomposition of $[Re_2(CO)_{10}]$ supported on mesoporous silica are shown in Figure 4. The $[Re_2(CO)_{10}]$

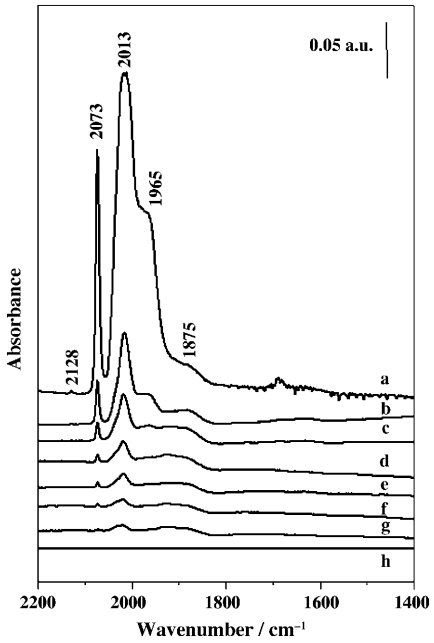

Figure 4. FTIR spectra of $[Re_2(CO)_{10}]$ anchored on silica at increasing outgassing temperature. a) 25, b) 100, c) 175, d) 225, e) 275, f) 300, g) 325, and h) 400 °C.

sample, which was outgassed at 25 °C (Figure 4, curve a), shows complex bands in the CO stretching region (2150–1800 cm^{-1}), and the intensity of these bands decreases when the temperature is progressively increased (Figure 4, curves b–g) and finally disappears when the outgassing is carried out at 400 °C (Figure 4, curve h). From Figure 4 it can be seen that the bands at $\tilde{\nu}=2128$ (weak), 2073 (strong), and 2013 (strong) with shoulders at 1965 and 1875 cm^{-1} (weak and broad) are present. It has been reported[15] that for an axially perturbed $[Re_2(CO)_{10}]$ molecule adsorbed on

a inorganic support, where the anchoring of metal carbonyls occurs through axial CO ligands, the point symmetry is C_{4v}. The C–O stretching representation is Γvib = 2E + B1 + B2 + 3A1, where the IR active modes are 2E + 3A1.[15] From this data, the bands at $\tilde{\nu}$ = 2128 and 2073 cm^{-1} can be assigned to the high frequency A1 modes, the band at 2013 cm^{-1} to the E mode, whilst the shoulder at 1965 cm^{-1} can be due either to the A1 or remaining E modes; these latter modes are observed possibly due to a modification of the axial symmetry. In addition to these modes, the weak and broad band present at $\tilde{\nu}$ = 1875 cm^{-1} can be attributed to a CO ligand that helps to anchor the complex to the silica support.[15,16]

In Figure 5, the FTIR spectra of $[Re_2(CO)_8(\mu\text{-}SbPh_2)_2]$ anchored to the silica support at increasing temperatures are presented. The spectrum of the sample outgassed at 25 °C (Figure 5, curve a) shows similar bands to the

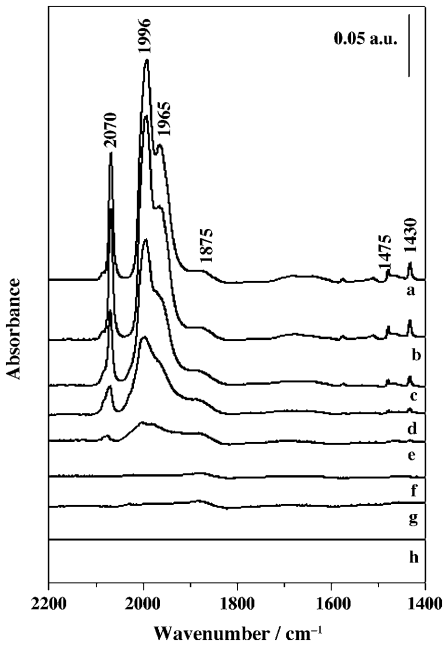

Figure 5. FTIR spectra of $[Re_2(CO)_8(\mu\text{-}SbPh_2)_2]$ anchored on silica at increasing outgassing temperature. a) 25, b) 100, c) 175, d) 225, e) 275, f) 300, g) 325, and h) 400 °C.

$[Re_2(CO)_{10}]$ cluster both in position and relative intensity observed in Figure 4, indicating the presence of the same carbonyls. The FTIR spectrum of this cluster precursor in hexane shows ν_{CO} bands at $\tilde{\nu}$ = 2067 (m), 1995 (vs) and 1960 cm^{-1} (s).[22] These bands can be assigned to the spectrum seen for the supported cluster prior to outgassing and heating. These bands, along with the weak bands at $\tilde{\nu}$ = 1475 and 1430 cm^{-1}, assigned to phenyl C–H bending modes, are removed after outgassing the sample at 300 °C (Figure 5, curve f). These results are in good agreement with the TGA that shows an inflection at around 280 °C (Figure 3, curve b). The only band to remain after outgassing at 300 °C is that at $\tilde{\nu}$ = 1875 cm^{-1}, assigned to the anchoring CO ligands.

The spectra related to the thermal decomposition of the $[Re_2(CO)_8(\mu\text{-}SbPh_2)(\mu\text{-}H)]$ complex are shown in Figure 6. The FTIR spectrum of the precursor complex in hexane

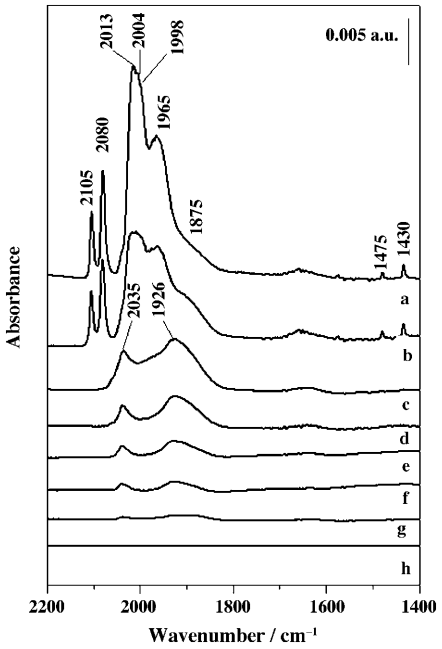

Figure 6. FTIR spectra of $[Re_2(CO)_8(\mu\text{-}SbPh_2)(\mu\text{-}H)]$ anchored on silica at increasing outgassing temperature. a) 25, b) 100, c) 175, d) 225, e) 275, f) 300, g) 325, and h) 400 °C.

shows ν_{CO} bands at $\tilde{\nu}$ = 2102 (w), 2078 (m), 2009 (s), 1997(s) and 1971 cm^{-1} (s). The typical bands of Re carbonyls present in the spectrum profile of the sample outgassed at 25 °C (Figure 6, curve a) are very similar to those of the precursor complex, with some shifts due to the sample environment and splitting due to the loss of symmetry of the anchored complex versus the complex in solution. A shoulder at $\tilde{\nu}$ = 1875 cm^{-1} is also present and is assigned to the stretching of the anchoring CO ligands. The weak bands in the 1500–1400 cm^{-1} range are related to the bending modes of CH groups of the phenyl ligands bonded to Sb. On heating sequentially to 225 °C (Figure 6, curve d), the ν_{CO} bands due to the precursor and the CH bands disappear in parallel, leaving ν_{CO} bands at $\tilde{\nu}$ = 2035 and 1926 cm^{-1}.

This indicates that the cluster initially anchors in a conformation similar to the structure of the precursor complex, by using hydrogen bonding between the surface silanol groups and CO ligands. On heating, the phenyl groups dissociate from the Sb, causing the Sb to bond to the surface and leaving the Re bound through anchoring CO ligands (1926 cm^{-1}).

Figure 7 shows the FTIR spectra of $[Re_2(CO)_8(\mu\text{-}BiPh_2)_2]$ on silica collected by outgassing at increasing temperature.

The FTIR spectrum of the precursor complex in hexane shows ν_{CO} bands at $\tilde{\nu}$ = 2064 (s), 1990 (vs) and 1960 cm^{-1} (s). This complex contains the same ligands and has a similar ge-

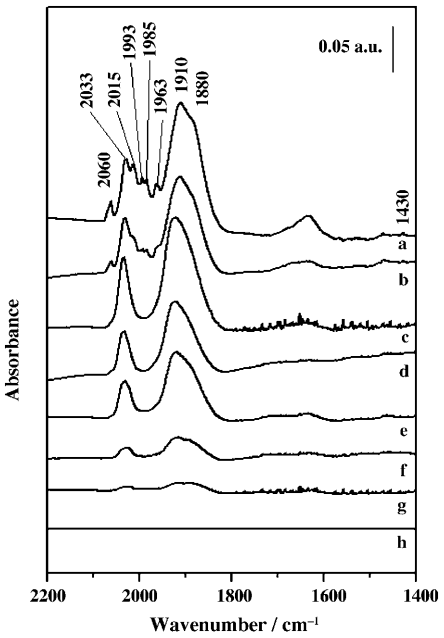

Figure 7. FTIR spectra of $[Re_2(CO)_8(\mu\text{-}BiPh_2)_2]$ anchored on silica at increasing outgassing temperature. a) 25, b) 100, c) 175, d) 225, e) 275, f) 300, g) 325, and h) 400 °C.

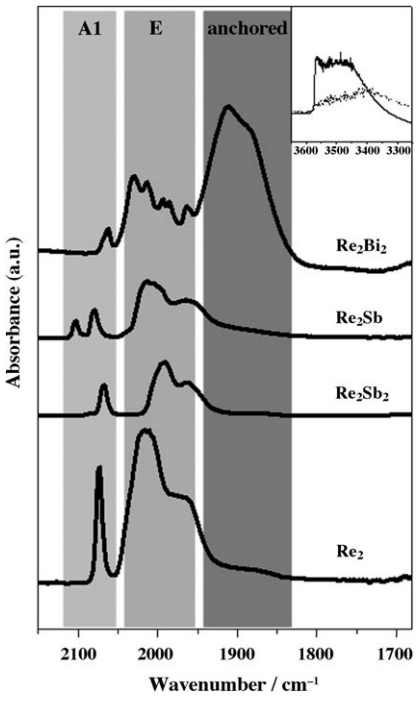

Figure 8. Main: FTIR spectra of $[Re_2(CO)_{10}]$, $[Re_2(CO)_8(\mu\text{-}SbPh_2)(\mu\text{-}H)]$, $[Re_2(CO)_8(\mu\text{-}SbPh_2)_2]$, and $[Re_2(CO)_8(\mu\text{-}BiPh_2)_2]$ anchored on silica. Inset: FTIR spectra in the OH stretching region of pure silica (solid line) and of $[Re_2(CO)_8(\mu\text{-}BiPh_2)_2]$ anchored on silica (dashed line). All the samples have been outgassed at room temperature.

ometry to that of the Re_2Sb_2; nevertheless the spectroscopic features are very different with respect to the other samples (see Figure 4–6). In particular, the spectrum of the complex outgassed at 25 °C appears more defined in the 2100–1950 cm^{-1} range. The fine structure of the spectrum contains bands that can be assigned to the precursor complex, with reduced symmetry due to distortion caused by interaction with the silica surface. The decomposition of the precursor as evidenced by the disappearance of the bands at $\tilde{\nu}=2060$, 2015, 1993, 1985 and 1963 cm^{-1} is complete at 175 °C (Figure 7, curve c); but three other bands ($\tilde{\nu}=2033$, 1910, and 1880 cm^{-1}) are still visible after degassing at 325 °C (Figure 7, curve g). Based on a strong evidence in the literature[15,16] and from its position and behavior, the features at 1910 and 1880 cm^{-1} can be assigned to the CO ligand anchoring the complex to the silica support. This band is present in all the as-synthesized samples, but its relative strength compared to the bands assigned to the undecomposed Re_2Bi_2 complex is much greater than for Re_2Sb and Re_2Sb_2, as evidenced in Figure 8, in which a comparison of the bands due to the different organometallic complexes on silica support is presented. The high relative intensity of this feature suggests that a greater proportion of Re_2Bi_2 decomposes to form nanoparticles at room temperature than in the case for Re_2Sb and Re_2Sb_2. This hypothesis is supported by the very weak absorption due to CH bending at $\tilde{\nu}=$ 1430 cm^{-1} (Figure 7, curve a).

The anchoring of the clusters through the silanol groups is further confirmed by looking at the spectra in the OH stretching region (see inset of Figure 8). In the case of neat silica, a broad absorption between 3800–3300 cm^{-1} is observed (solid line in the inset) after outgassing the sample at room temperature. Although, this absorption is complex, it is possible to pick up a band at $\tilde{\nu}=3745$ cm^{-1}, which is due to the stretching mode of free silanols, and a broad absorption at lower wavenumbers, extending to $\tilde{\nu}=3300$ cm^{-1}, due to hydrogen bonding between silanols and other Si–OH groups or chemisorbed water that is not removed at room temperature. On anchoring of the organometallic complex containing Bi (Figure 8, dashed line in the inset), the band associated with the silanol groups displays very low intensity (the spectra are normalized) and this indicates that the concentration of SiOH groups is low. From the above, we can infer that the disappearance of these silanol bands indicates that the SiOH are the locus at which the anchoring occurs. The same behavior is observed when a different complex, for example $[TiCl_2Cp_2]$ (Cp = cyclopentadienyl), is anchored on mesoporous silica.[17,18]

Moreover, the comparison of Re_2Sb and Re_2Sb_2 samples in Figure 8 reveals that not only the band ascribed previously to the A1 mode, but also the component due to the E mode is split in the case of Re_2Sb, due to the decrease in the symmetry of the complex with respect to pure Re. These modes are slightly red shifted in the case of Re_2Sb_2, where the splitting is not observed, due to its different geometry. Based on the decomposition of the ν_{CO} bands of the supported, undecomposed complexes, comparison of the spectra for the three bimetallic clusters indicates an order of stability to vacuum thermolysis of $Re_2Sb_2 > Re_2Sb > Re_2Bi_2$.

Of the three catalyst samples, only the FTIR spectra of Re_2Bi_2 show full decomposition of the precursor complex bands when activated at 200 °C prior to the catalytic tests, which could well explain the superior performance of this catalyst[11] (see Figure 2).

The FTIR spectra of the as-synthesized samples have shown that the interaction between the support and the organometallic complex is very strong in the case of Re_2Bi_2 as evidenced by the intense absorption at lower frequency due to anchored CO sites (Figure 8). This kind of interaction strongly affects the nature of the metal nanoparticles that are formed after the decomposition of the precursors and form the loci at which the resulting catalysis ensues. To explore the effect of the thermal treatment on the production of the active sites and to elucidate the nature of the metal nanoparticles formed on the silica support, CO adsorption at room temperature was performed on the catalysts activated both at 200 °C and at 400 °C. These temperatures were specifically chosen because catalytic tests have been normally performed on nanoparticle catalysts that have been activated in the 200–300 °C temperature range,[11] whilst in the previous section we have shown that an activation temperature of 400 °C is necessary in the case of Re_2Sb and Re_2Sb_2 in order to completely remove all the carbonyl species.

In Figure 9 A the FTIR spectra of CO irreversibly adsorbed on the Re_2Sb, Re_2Sb_2, and Re_2Bi_2 catalysts activated at 200 °C are reported. No evidence of CO absorption on either Bi or Sb sites was observed and all the absorptions indicating CO interaction are due to CO molecules adsorbed on rhenium centers. CO interaction on the Re_2Sb catalyst produced a large number of intense (the absorbance for this spectrum is divided by a factor of 4) and quite definite bands at $\tilde{\nu}=2130$, 2062, 2039, 2010, and 1967 cm^{-1}. The 2130 cm^{-1} band is typical for the stretching mode of CO molecules adsorbed on partially reduced Re^{n+} sites, which indicates the presence of Re in higher oxidation states.[19] At lower wavenumber, a series of bands are present that are due to CO adsorbed on reduced rhenium sites, which are coordinated differently and probably still interacting with the residual ligands of the cluster. It is worth noting here that a negative band at $\tilde{\nu}=1923$ cm^{-1} is observed, which can be attributed to anchoring CO in the decomposition spectra (1926 cm^{-1}, Figure 6), although the intensity of the negative band is much greater to that seen in Figure 6. The presence of a residual fraction of undecomposed complex, at this activation temperature, is observed in the FTIR spectra related to the decomposition of the precursor (Figure 6). In addition, this behavior is also an indication that CO is able to remove the residual species at room temperature. A negative band in the same position is also observed for Re_2Bi_2, which is also in the same position as the anchoring CO band in Figure 7, but unlike Re_2Sb it is of lower intensity. This negative band is not observed in the Re_2Sb_2 spectrum, although it should be noted from Figure 5 that after degassing at 225 °C, the decomposition spectra of Re_2Sb_2 contained the weakest band due to anchoring CO of any of the tested species. These differences can be explained by considering

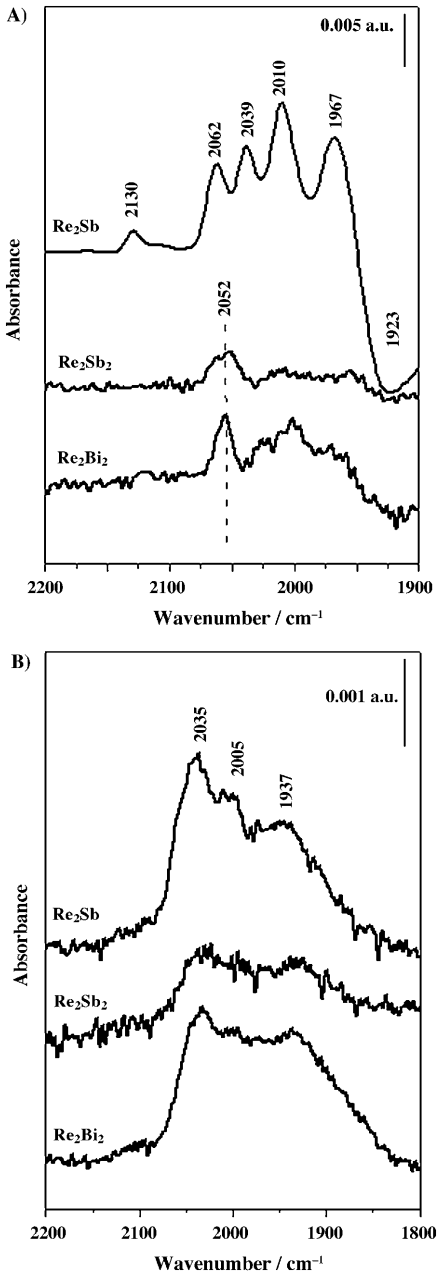

Figure 9. FTIR spectra recorded after the CO adsorption and subsequent outgassing at room temperature on Re_2Sb, Re_2Sb_2, and Re_2Bi_2 catalysts activated in vacuo at A) 200 and B) 400 °C.

that on Re_2Sb_2 all ligands are removed between 225 and 275 °C (Figure 5, curves d and e), whereas on Re_2Sb and Re_2Bi_2 weak bands due to residual ligand are still visible up to 325 °C (curve g in Figure 6 and 7).

In the case of Re_2Sb_2 and Re_2Bi_2, only weak bands are formed upon CO adsorption at room temperature. In particular, a band at $\tilde{\nu}=2052$ cm^{-1} is observed for both samples that can be specifically assigned to CO adsorbed on well dispersed Re^0 sites.[19–21] A weak band in the same position was observed by adsorbing CO on pure Re_2 sample (see the Supporting Information). The band at $\tilde{\nu}=2052$ cm^{-1} appears

quite symmetric in the case of Re_2Bi_2 indicating the presence of well-defined single-site Re^0 exposed at the surface of the metal nanoparticles, thus, the presence of oxophilic atoms is essential to obtain single-site Re^0 centers. In fact, the Re_2 sample shows only a small amount of Re^0 sites after the precursor decomposition, as evidenced by the presence of the weak band at approximately $\tilde{\nu}=2052\ cm^{-1}$ (see Figure 1 in the Supporting Information).

CO adsorption was also performed on the catalysts activated at 400 °C in order to monitor the nature of the metal-exposed sites after complete removal of the ligands (Figure 9B) and the disappearance of the negative bands was clearly evident in all cases. A decrease in the overall intensity and a red shift of the CO bands was observed with respect to the spectra of the catalysts activated at 200 °C, suggesting a lower fraction of available Re^0 sites and their modification under these thermal conditions. In particular, the band at $\tilde{\nu}=2130\ cm^{-1}$, due to Re^{n+} sites, present in the Re_2Sb catalyst activated at 200 °C, and the band at $\tilde{\nu}=2052\ cm^{-1}$, due to well-dispersed Re^0 single sites, present on Re_2Bi_2 and Re_2Sb_2 catalysts have completely disappeared. These data suggest that an higher thermal treatment is necessary to completely reduce the oxidized Re sites present on the Re_2Sb catalyst and that the nature of the Re^0 single sites, formed especially on Re_2Bi_2 and Re_2Sb_2 samples activated at 200 °C, has been modified after the thermal treatment at 400 °C.

These results further confirm that the nature of the oxophilic metal and the temperature of activation clearly play an important role in the generation of isolated, well-defined single sites, which are crucial for the catalytic activity (see Figure 2). When the three rhenium-based nanocluster catalysts were activated at 200 °C, the presence of oxidized Re^{n+} sites had a detrimental effect on the catalytic efficiency of the Re_2Sb catalyst. Further, it is also clear from Figure 2, that Bi is a better oxophile when alloyed with Re, and the fact that there is a larger proportion of the undecomposed precursor still present in the Re_2Sb_2 when compared to Re_2Bi_2 at 200 °C (compare Figure 5 and 7) could well explain the superior performance of the Re_2Bi_2 catalyst. Higher activation temperatures (400 °C) were employed to completely remove all the precursor ligands; but this had a detrimental effect on the catalysis, as the isolated Re^0 single sites were destroyed at this temperature (see Figure 9B) possibly due to sintering or coke formation.

Conclusion

FTIR spectroscopy and thermogravimetric analysis (TGA) have exemplified that the decomposition of rhenium-containing organometallic precursors occurs at different temperatures, clearly illustrating that the nature of the oxophilic metal (Sb or Bi) and the geometry of the cluster complex play a major role in influencing the stability of the nanocluster catalyst and, thereby, its catalytic properties. The interaction between the organometallic cluster complexes and the silica support is the driving force that leads to the production of Re^0 single sites, which are active for the ammoxidation of 3-picoline. The key step in the decomposition of the precursor complexes is the loss of the phenyl groups from the oxophile and its subsequent binding to the silica surface. The nanoparticles that are generated from this step do not undergo any modification until all the CO ligands are removed; including any CO anchoring the Re atoms to the silica, as evidenced by the consistent shapes of the IR spectra of the anchored nanoparticles. In the case of the Re_2Bi_2 catalyst, in which the largest fraction of anchored CO sites are present, well-defined Re^0 single sites exposed at the surface are observed, as evidenced by the CO adsorption, and this catalyst displays the highest catalytic activity for the ammoxidation of 3-picoline at 200 °C. The Re^0 single sites are extremely sensitive to the thermal treatment and higher activation temperatures (400 °C) strongly modify these nanocluster catalysts, which leads to the complete disappearance of the bands associated with the Re^0 sites. This is evidenced (Figure 2) by the poor performance exhibited by these catalysts and it could well be envisaged that higher activation temperatures lead to aggregation followed by subsequent sintering of the nanoparticles or coke formation. Further work by using X-ray absorption spectroscopy (EXAFS and XANES) is in progress to elucidate the above.

Experimental Section

The organometallic precursor complexes were anchored onto a mesoporous silica support (Grace Davison, designated Davison 911, having a pore diameter of 38 Å) by using CH_2Cl_2 as the solvent (ca. 3% metal loading). The solvent was removed under a slow stream of nitrogen. The pure rhenium (denoted as Re_2) and the pure bismuth samples were prepared similarly on Davison 911 mesoporous silica by using a commercially obtained [$Re_2(CO)_{10}$] and [$BiPh_3$] as the precursors. The catalysts were activated by heating the supported clusters to the desired temperature (200 or 400 °C) in vacuo for 2 h. The catalytic tests were performed in a high-pressure stainless reactor lined with poly(ether ether ketone) (PEEK). The catalysts were reduced for 1 hour at 200 °C under an atmosphere of H_2 (20 bar), prior to the introduction of the substrate. The reactor was then depressurized and cooled to room temperature, before introducing the 3-picoline (5.0 g) and solvent (toluene, 25 mL). After introducing the reactant and the internal standard (tetralin, 100 mg), the reactor was purged thrice with dry nitrogen prior to the introduction of NH_3 (20 bar) and air (40 bar). During the reaction, small aliquots were removed by using a mini-robot autosampler to enable the kinetics to be studied. The products of the reaction were analyzed with gas chromatography (G.C. Varian Model 3400 CX) employing a HP-1 capillary column (25 m × 0.32 mm) and flame ionization detector. The identity of the products was further confirmed by using LC-MS (Shimadzu LCMS-QP8000), which was again employed either online or offline. The conversions, the selectivities, and the turnover number (TON) were determined as defined by Equations (1)–(3) and the yields were normalized with respect to the response factors obtained as above:

$$\text{conv.}\% = \left[\frac{\text{mol}_{\text{initial substrate}} - \text{mol}_{\text{residual substrate}}}{\text{mol}_{\text{initial substrate}}}\right] \times 100 \quad (1)$$

$$\text{sel.}\% = \left[\frac{\text{mol}_{\text{individual product}}}{\text{mol}_{\text{total products}}}\right] \times 100 \quad (2)$$

$$\mathrm{TON} = \left[\frac{\mathrm{mol}_{\mathrm{substrat\ conv.}}}{\mathrm{mol}_{\mathrm{cluster}}}\right] \tag{3}$$

For the internal standard GC method, the response factor (RF) and mol% of individual products were calculated by using Equation (4):

$$\begin{aligned}\mathrm{RF} &= \frac{\mathrm{mol}_{\mathrm{product}}}{\mathrm{mol}_{\mathrm{standard}}} \times \frac{\mathrm{area}_{\mathrm{standard}}}{\mathrm{area}_{\mathrm{product}}}\ \mathrm{mol\%}_{\mathrm{product}} \\ &= \mathrm{RF} \times \mathrm{mol}_{\mathrm{standard}} \times \frac{\mathrm{area}_{\mathrm{product}}}{\mathrm{area}_{\mathrm{standard}}} \times \frac{100}{\mathrm{mol}_{\mathrm{sample}}}\end{aligned} \tag{4}$$

Thermogravimetric analysis of the as-synthesized samples was performed on a Setaram SETSYS Evolution Instrument with a heating rate of $5\,^{\circ}\mathrm{C\,min^{-1}}$ up to 500 °C in an Ar flow ($20\,\mathrm{mL\,min^{-1}}$). FTIR spectra of self-supporting wafers of the samples (ca. $5\,\mathrm{mg\,cm^{-2}}$) were recorded with a Bruker IFS88 spectrometer at a resolution of $4\,\mathrm{cm^{-1}}$. The as-synthesized samples were outgassed and heated to the desired temperature in vacuo. CO was adsorbed at room temperature on the activated samples by using specially designed cells that were permanently connected to a vacuum line (ultimate pressure $< 10^{-5}$ Torr) to perform the in situ adsorption–desorption experiments. CO adsorption was performed at room temperature to eliminate the contribution of the silica support. FTIR spectra were reported in difference mode and in the case of as-synthesized samples, the difference spectra were obtained by subtracting the spectrum of the sample after the complete decomposition of the complex from that of the anchored organometallic complexes. The spectra of adsorbed CO were obtained by subtracting the spectrum of the sample pre-adsorption from the spectrum with adsorbed CO. CO was also adsorbed on the catalysts after activation in vacuo at 200 °C and at 400 °C for 2 h.

Acknowledgements

We thank the National Science Foundation under Grant No. CHE-0743190 and the British Italian Partnership Program and EPSRC (UK) for financial support. The authors are also grateful to Compagnia di San Paolo for sponsorship to NIS—Centre of Excellence (Torino) and to Dr. C. Bisio for TGA.

[1] W. A. Herrmann, R. W. Fischer, D. W. Marz, *Angew. Chem.* **1991**, *103*, 1706–1709; *Angew. Chem. Int. Ed.* **1991**, *30*, 1638–1641.

[2] A. W. Moses, C. Raab, R. C. Nelson, H. D. Leifeste, N. A. Ramsahye, S. Chattopadhyay, J. Eckert, B. F. Chmelka, S. L. Scott, *J. Am. Chem. Soc.* **2007**, *129*, 8912–8920.

[3] Y. Yuan, Y. Iwasawa, *J. Phys. Chem. B* **2002**, *106*, 4441–4449.

[4] W. A. Herrmann, *Angew. Chem.* **1988**, *100*, 1269–1286; *Angew. Chem. Int. Ed. Engl.* **1988**, *27*, 1297–1313.

[5] J. Sundermeyer, *Angew. Chem.* **1993**, *105*, 1195–1197; *Angew. Chem. Int. Ed. Eng.* **1993**, *32*, 1144–1146.

[6] M. Gaigneaux, H. Liu, H. Imoto, T. Shido, Y. Iwasawa, *Top. Catal.* **2000**, *11*, 185–193.

[7] H. Liu, H. Imoto, T. Shido, Y. Iwasawa, *J. Catal.* **2001**, *200*, 69–98.

[8] H. Liu, M. Gaigneaux, H. Imoto, T. Shido, Y. Iwasawa, *Catal. Lett.* **2001**, *71*, 75–79.

[9] H. S. Lacheen, P. J. Cordeiro, E. Iglesia, *J. Am. Chem. Soc.* **2006**, *128*, 15082–15083.

[10] R. J. Lobo-Lapidus, M. J. McCall, M. Lanuza, S. Tonnesen, S. R. Bare, B. C. Gates, *J. Phys. Chem. C* **2008**, *112*, 3383–3391.

[11] R. Raja, R. D. Adams, D. A. Blom, W. C. Pearl, Jr., E. Gianotti, J. M. Thomas, *Langmuir* **2009**, *25*, 7200–7204.

[12] R. D. Adams, B. Captain, W. C. Pearl, Jr., *J. Organomet. Chem.* **2008**, *693*, 1636–1644.

[13] J. M. Thomas, R. D. Adams, E. M. Boswell, B. Captain, H. Gronbeck, R. Raja, *Faraday Discuss.* **2008**, *138*, 301–315.

[14] R. D. Adams, E. M. Boswell, B. Captain, A. B. Hungria, P. A. Midgley, R. Raja, J. M. Thomas, *Angew. Chem.* **2007**, *119*, 8330–8333; *Angew. Chem. Int. Ed.* **2007**, *46*, 8182–8185.

[15] C. Mas Carbonell, C. Otero Areàn, *Vib. Spectrosc.* **1996**, *12*, 103–107.

[16] C. J. Papile, B. C. Gates, *Langmuir* **1992**, *8*, 74–79.

[17] E. Gianotti, V. Dellarocca, L. Marchese, G. Martra, S. Coluccia, T. Maschmeyer, *Phys. Chem. Chem. Phys.* **2002**, *4*, 6109–6115.

[18] M. E. Raimondi, E. Gianotti, L. Marchese, G. Martra, T. Maschmeyer, J. M. Seddon, S. Coluccia, *J. Phys. Chem. B* **2000**, *104*, 7102–7109.

[19] W. Daniell, .T. Weingand, H. Knozinger, *J. Mol. Catal. A* **2003**, *204–205*, 519–526.

[20] F. Solymosi, T. Bànsàgi, *J. Phys. Chem.* **1992**, *96*, 1349–1355.

[21] M. Komiyama, J. Sato, K. Yamamoto, Y. Ogino, *Langmuir* **1987**, *3*, 845–851.

[22] R. D. Adams, M. B. Hall, W. C. Pearl, X. Z. Yang, *Inorg. Chem.* **2009**, *48*, 652–662.

Received: November 11, 2009
Published online: June 8, 2010

